



Magnetic nanoparticles for removing inorganic arsenic species from waters: A proof of concept for potential application

Yesica Vicente-Martínez^a, Manuel Caravaca^b, Sokaina El Farh^a, Manuel Hernández-Córdoba^a, Ignacio López-García^{a,*}

^a Department of Analytical Chemistry, Faculty of Chemistry, Regional Campus of International Excellence "Campus Mare Nostrum", University of Murcia, Murcia 30100, Spain

^b University Centre of Defence at the Spanish Air Force Academy, c/ Coronel López Peña s/n, San Javier 30720, Spain

ARTICLE INFO

Keywords:

Inorganic arsenic removal
Magnetic separation
Ferrite
Electrothermal atomic absorption spectrometry

ABSTRACT

Inorganic arsenic is considered one of the most critical and severe environmental problems due to its high toxicity even at low levels of exposure, causing serious health problems. Humans can be exposed to arsenic mainly through inhalation, ingestion of food and water, especially in certain areas where water comes into contact with arsenic-bearing minerals. For natural geological reasons, water in some areas of the world may contain more arsenic than usual. For these circumstances, the development of methods for the removal of arsenic from water has been of increasing interest in recent years. This work presents an optimised removal of As(III) and As(V) from water by the *in situ* formation of ferrite (Fe₃O₄) nanoparticles, leading to the adsorption of this element in the Fe₃O₄ structure. In addition, the magnetic properties of the nanoparticles facilitate their removal from the medium by a magnet. The experimental conditions of the process were optimised and the total removal of high concentrations of As(III) and As(V) in water was achieved in only two minutes and at 50 °C at basic pH, using 200 µL of a 0.2 M FeCl₂·4H₂O solution and 100 µL of a 0.1 M FeCl₃·6H₂O solution to form Fe₃O₄ *in situ*. The ferrite surface was characterised by field emission scanning electron microscopy before and after the arsenic removal process and by energy dispersive X-ray spectroscopy before the process. The study of adsorption kinetics and equilibrium isotherms reveals a Langmuir-type physicochemical process.

1. Introduction

Arsenic is a highly persistent element with a high tendency to accumulate in fatty tissues. It is also one of the most toxic and carcinogenic metalloids found in the environment [1]. For these reasons, the presence of As in water has received considerable attention worldwide in recent years and has become a global environmental problem of major concern [2]. During the last decade, numerous studies have been carried out in several affected countries where water systems are in need of arsenic abatement in order to comply with the World Health Organisation (WHO) guidelines for drinking water supply [3]. In this regard, a compilation of regulations on arsenic content in drinking water from many national governments around the world has recently been published [4].

Arsenic is present in the environment as a result of various anthropogenic, biogenic and geogenic activities, with different toxicity depending on the oxidation state, As(III) being more toxic than As(V) and the latter being more toxic than organic species of arsenic [5]. Because of the severe consequences for human health caused by the presence

of the most toxic species of As, the WHO has restricted the maximum concentration of arsenic in drinking water to 10 µg L⁻¹ [3].

The high toxicity of As(III) and As(V) has led to the development of numerous methods to remove this metalloid from water over time, with the most commonly used traditional methods being based on chemical precipitation, electrochemical treatment or ion exchange [6]. Arsenic adsorption using activated carbon has also been widely used. However, these traditional methods are not efficient enough, especially when As concentrations are not very high [7]. For this reason, much research has been carried out in recent years with the aim of removing As from water with a high removal efficiency, even at low concentrations. Recently, the use of different adsorptive membranes based on different materials has been addressed, in particular those based on sulfonates, with a maximum removal efficiency of 72% achieved under reduced pressure, or those based on metal-organic frameworks, which achieve up to 87% arsenic removal [8]. Remarkably, membranes based on graphene oxide have reached 99% of arsenic removal efficiency, although the overall removal process is slow, needing 24 h of contact time [9].

* Corresponding author.

E-mail address: ilgarcia@um.es (I. López-García).

Table 1
Furnace program.

Stage	Temperature, °C	Ramp, s	Hold, s
Dry	110	5	20
Dry	130	5	20
Ash	900	10	30
Atomisation ^a	2200	0	5
Clean	2450	1	3

^a Reading stage. The inner gas flow was stopped.

Arsenic removal by adsorption processes has also been extensively studied in recent years. A wide variety of materials have been used to remove both As(III) and As(V) from water, such as persulfate compounds, achieving 96% removal efficiency with the need for a UV lamp to produce the oxidation of As [10]. A graphene-oxide-iron nanohybrid has been used to remove arsenic from water with excellent results in about 10 min, but the synthesis of the adsorbent requires appropriate technology [11]. In addition, a TiO₂/FeOOH-based hybrid material has been used, resulting in an efficiency of 96%, although this process requires at least 12 h to complete [12].

In this work, a novel method has been developed for the simultaneous removal of As(III) and As(V) in water through the in situ formation of magnetic ferrite nanoparticles. This procedure is on the one hand, a proof of concept to study its application in larger sample volumes, adjusting the conditions to achieve greater efficiency, and on the other hand, because it is a microsolid-phase extraction, it could be used for the subsequent quantification of arsenic traces. The adsorbent material used is very cheap and also has properties that allow its rapid formation in an aqueous medium, leading to the instantaneous adsorption of arsenic and its subsequent removal from the medium by the action of a magnet. The optimal experimental conditions and the thermodynamics of the process have been studied. In addition, the adsorbent material has been characterised by field emission scanning electron microscopy before and after the arsenic removal process and by energy dispersive X-ray spectroscopy after the process. The process proposed in this work represents a great alternative in the removal of arsenic from water due to its simplicity, cost effectiveness and speed.

2. Materials, instruments and procedure

2.1. Reagents and instrumentation

In this work, all reagents used in the experiments were of analytical grade. Standard solutions of As(III) and As(V) at a concentration of 1000 mg L⁻¹ provided by Merck (Darmstadt, Germany) were used to prepare the dilute solutions of arsenic species. The nitric acid used was purchased from Panreac (Barcelona, Spain) and for the synthesis of ferrite (Fe₃O₄) as adsorbent material, the following reagents from Merck were used: ammonium hydroxide, FeCl₃·6H₂O and FeCl₂·4H₂O. In addition, an ultrasonic thermostated bath Labbox model ULTR (Barcelona, Spain) was used to synthesise Fe₃O₄. An atomic absorption spectrometer model AAnalyst 600 from Perkin-Elmer (Waltham, Massachusetts, USA) equipped with integrated platform transversely-heated graphite tube and arsenic electrodeless discharge lamp were used to measure the arsenic signal in the solutions. The heating program appears on Table 1.

2.2. In situ preparation of Fe₃O₄ nanoparticles and arsenic removal procedure

To 10 mL of an aqueous solution containing As(III) and As(V) in a total concentration lower than 200 µg L⁻¹, 200 µL of FeCl₂·4H₂O (0.2 M) solution and 100 µL of FeCl₃·6H₂O (0.1 M) solution were added. After manual shaking, 50 µL of concentrated ammonia solution was added to form the nanoparticles according to the following reaction [13]:

Table 2
Amount of ferrite formed in relation to the volume of precursor solutions added.

µL of FeCl ₂ ·4H ₂ O solution	µL of FeCl ₃ ·6H ₂ O solution	mg of Fe ₃ O ₄	Removal ^a , %
50	25	0.5 ± 0.2	54 ± 3
100	50	1.2 ± 0.2	83 ± 4
200	100	2.4 ± 0.1	101 ± 4
300	150	3.6 ± 0.1	99 ± 5

^a mean value ± standard deviation (n = 3).



The mixture was then placed in a thermostatic bath at 50 °C for 3 min. When the reactants come into contact, the formation of Fe₃O₄ is instantaneous and a magnetic brown precipitate appears. As the nanoparticles are formed, the arsenic atoms present in the aqueous solution are adsorbed onto them. As the nanoparticles are magnetic, they are easily removed from the medium by the action of a magnet. In this way, the arsenic is removed from the aqueous medium together with the nanoparticles.

3. Results and discussion

3.1. Characterization of Fe₃O₄ before and after arsenic removal

The ferrite nanoparticles (Fe₃O₄) were characterised after their synthesis in an arsenic-free water sample by field emission scanning electron microscopy (FESEM) imaging, as shown in Fig. 1. In addition, Fig. 2 shows the Energy Dispersive X-Ray (EDX) spectrum corresponding to the whole area of the image shown in Fig. 1, together with its atomic concentration table, which shows strong signals for Fe and O atoms, as expected.

Subsequently, after the As removal process in water, the magnetic adsorbent was again characterised to show the presence of arsenic retained on the Fe₃O₄. Fig. 3 shows the backscattered electron (BSE) analysis of the adsorbent after the As removal process. It is necessary to use this technique because the concentration of As is very low and cannot be visualised by standard FESEM analysis. BSE was able to distinguish the arsenic atoms as brighter structures on the adsorbent due to their high atomic number [14,15]. Consequently, Fig. 3 shows brighter areas corresponding to As adsorbed on Fe₃O₄, although it is not possible to distinguish between the arsenic species.

3.2. Effect of Fe₃O₄ dose on arsenic removal

To achieve maximum removal of As(III) and As(V) in aqueous solution, the required dose of Fe₃O₄ was investigated. For this purpose, the removal of both arsenic species was studied separately. In 10 mL of aqueous solution containing a concentration of 50 µg L⁻¹ As, the removal process was carried out using different amounts of precursor (Table 2). The amount of ferrite obtained using these volumes is also shown in Table 2. As can be seen, amounts of magnetic adsorbent of 0.5, 1.2, 2.4 and 3.6 mg were obtained.

For both As species, the best results were obtained with a ferrite dose of 2.4 mg, obtained by adding 200 µL of FeCl₂·4H₂O (0.2 M) and 100 µL of FeCl₃·6H₂O (0.1 M) solutions.

3.3. Contact time effect on arsenic species removal and effect of pH

The contact time between the Fe₃O₄ nanoparticles and the aqueous solution containing the arsenic ions was studied to obtain maximum As removal for times equal to 0, 1, 2, 5 and 10 min. The 0 value corresponds to the application of the magnet just when the nanoparticle precursors are added to the aqueous solution and the brown precipitate appears.

Both arsenic species behaved similarly and showed exceptional removal rates, reaching 91% for As(III) and 96% for As(V) at 0 min and

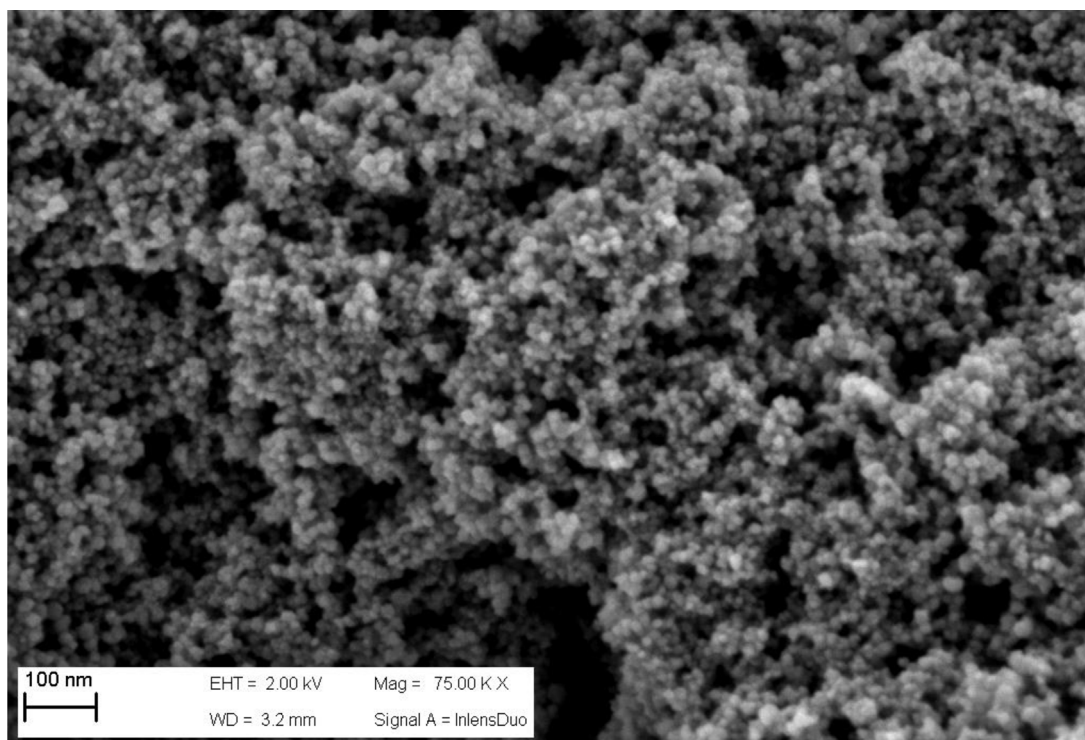
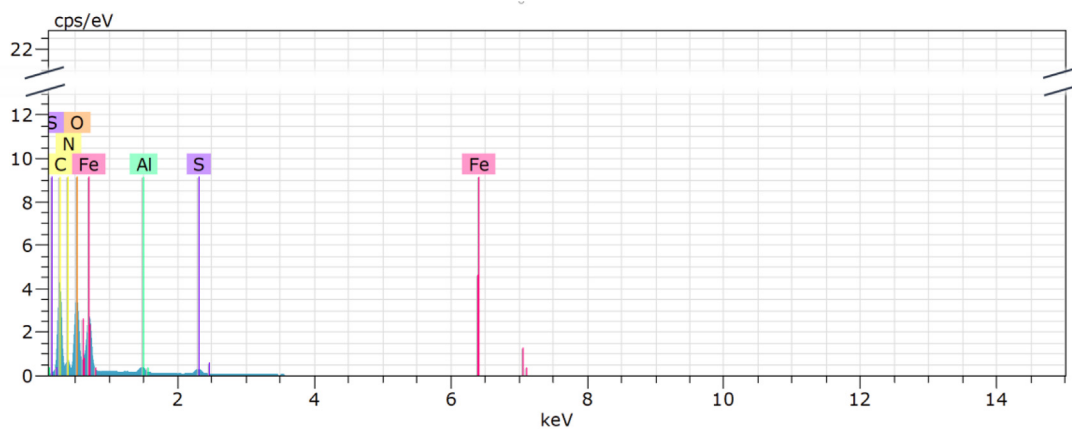


Fig. 1. FESEM image for Fe₃O₄ synthesized in arsenic-free aqueous solution.



E1	AN	Series	Unn [wt, %]	C norm. [wt, %]	C Atom. [at, %]	C Error [wt, %]
C	6	K-series	22.50	22.50	40.31	2.63
N	7	K-series	5.87	5.87	9.01	0.84
O	8	K-series	21.81	21.81	29.33	2.55
Al	13	K-series	2.08	2.08	1.66	0.13
S	16	K-series	4.53	4.53	3.04	0.26
Fe	26	L-series	43.20	43.20	16.64	5.02
Total:			100.00	100.00	100.00	

Fig. 2. (EDX) spectrum (top) and atomic concentration table with (bottom) for Fe₃O₄ (whole area of Fig. 1) synthesized in arsenic-free aqueous solution.

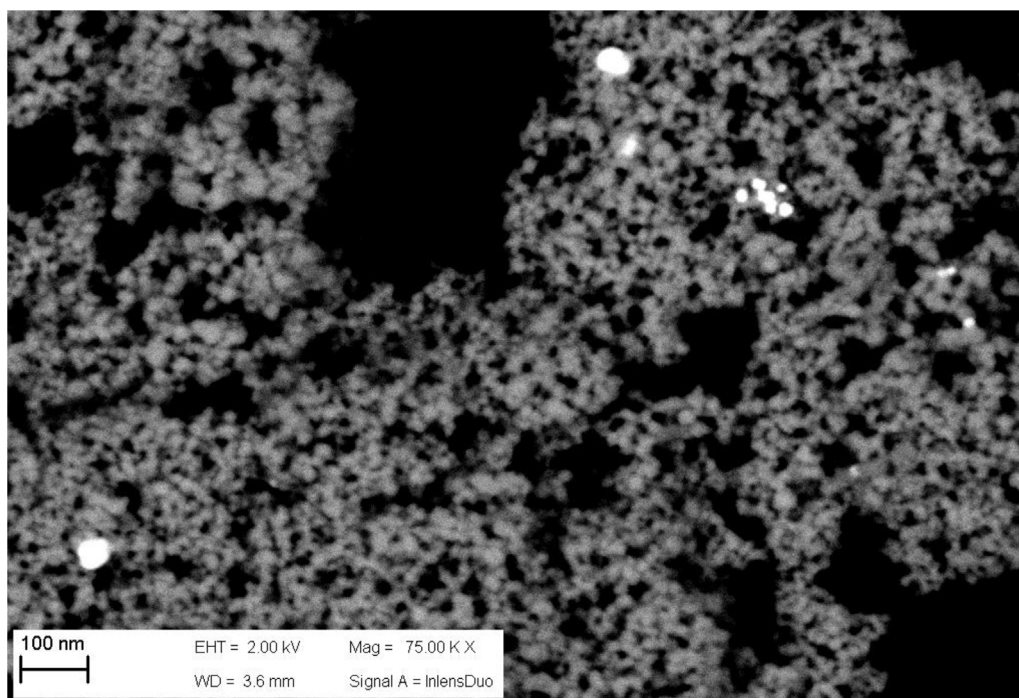


Fig. 3. BSE images of Fe_3O_4 after arsenic removal, displaying brighter structures which corresponds to As adsorbed onto Fe_3O_4 .

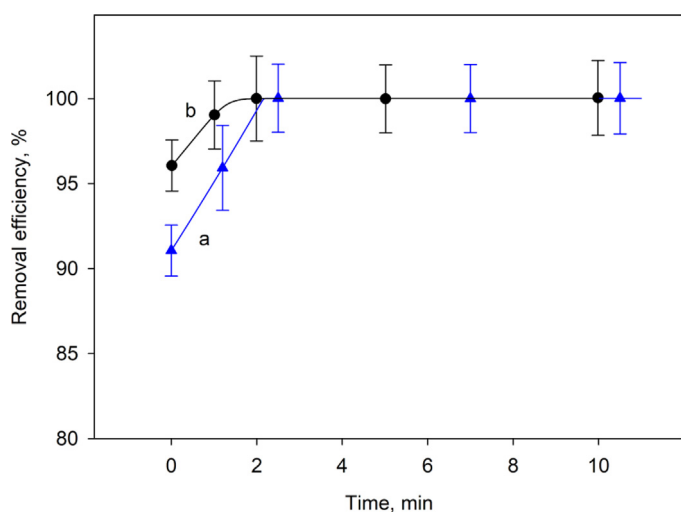


Fig. 4. Dependence of the removal efficiency of As(III) and As(V), curves a and b, respectively, on the contact time. Saturation to the maximum removal efficiency occurs at 2 min, for both As species. Error bars correspond to the standard deviation of three determinations.

96% for As(III) and 99% for As(V) after 1 min contact time. The optimum time chosen to ensure that all As species present in the water solution were removed was 3 min. The results are shown in Fig. 4. The error bars correspond to the standard deviation of three experiments. Due to the rapidity of the removal process and the rapid saturation to maximum removal efficiency, no further kinetic characterisation is possible and the data do not fit kinetic models such as pseudo-first order, pseudo-second order, hybrid, Elovich or intraparticle diffusion.

In the process of ferrite nanoparticle formation, a basic pH is required, so that considering the pK_a values of H_3AsO_4 (2.20, 6.97 and 11.53) and H_3AsO_3 (9.22, 12.13 and 13.4) [16], the negatively charged arsenic species predominate, suggesting that the interaction with the atoms conforming the ferrite structure may be electrostatic in nature

with the positively charged Fe atoms in the aqueous solution, prior to the formation of Fe_3O_4 , thus encapsulating the As in the adsorbent structure. This would explain the instantaneous disappearance of virtually all As ions from the aqueous solution during ferrite formation.

After the adsorption of arsenic on ferrite it is necessary to separate the aqueous phase from the adsorbent material. This is quickly achieved with the use of a neodymium magnet. We have used a permanent magnet of Nd-Fe-B ($50 \times 15 \times 15$ mm) of 86 g and with a force of 33 kg, which allows the complete separation of the solid phase in 10 mL of solution in less than 1 min.

3.4. Study of adsorption isotherms and the effect of the process temperature

Adsorption isotherms were characterized independently for As(III) and As(V) at temperatures 293, 303, 323 and 343 K, relating the equilibrium adsorption capacity q_e (mg g^{-1}) and the equilibrium adsorbate concentration C_e (mg L^{-1}). Isotherm corresponding to 343 K matched that of 323 K, since their removal efficiencies were 100% for all C_e values. Adsorbent concentrations C_e were 50, 100, 150 and 200 ppb, for all the temperatures. Adsorption isotherm model selected was Langmuir [17], which considers homogenous monolayer adsorption, giving rise to the best fitting results (adjusted $R^2 > 0.99$), over others such as Freundlich or Temkin isotherms [18], which offered worse statistics (adjusted $R^2 < 0.98$). Langmuir model relates q_e and C_e as follows:

$$\frac{1}{q_e} = \frac{1}{q_m} + \frac{1}{K_L q_m C_e} \quad (1)$$

In Eq. (1), K_L is the Langmuir adsorption constant (L mg^{-1}) and q_m is the maximum adsorption capacity of the adsorbent (mg g^{-1}). Adjusted R^2 values and reduced χ^2 for As(III) and As(V), as long as K_L constants are shown in Table 3 for the temperatures under study (Fig. 5).

As stated above, the Langmuir model gave the best fitting results over other models such as Freundlich or Temkin, but to make a deeper comparison, statistical tests computed in Origin 2022, specifically Akaike's and Bayesian information criteria (AIC and BIC, respectively), were performed, both concluding that the Langmuir model is more likely to describe the equilibrium adsorption of As on Fe_3O_4 . AIC and BIC values

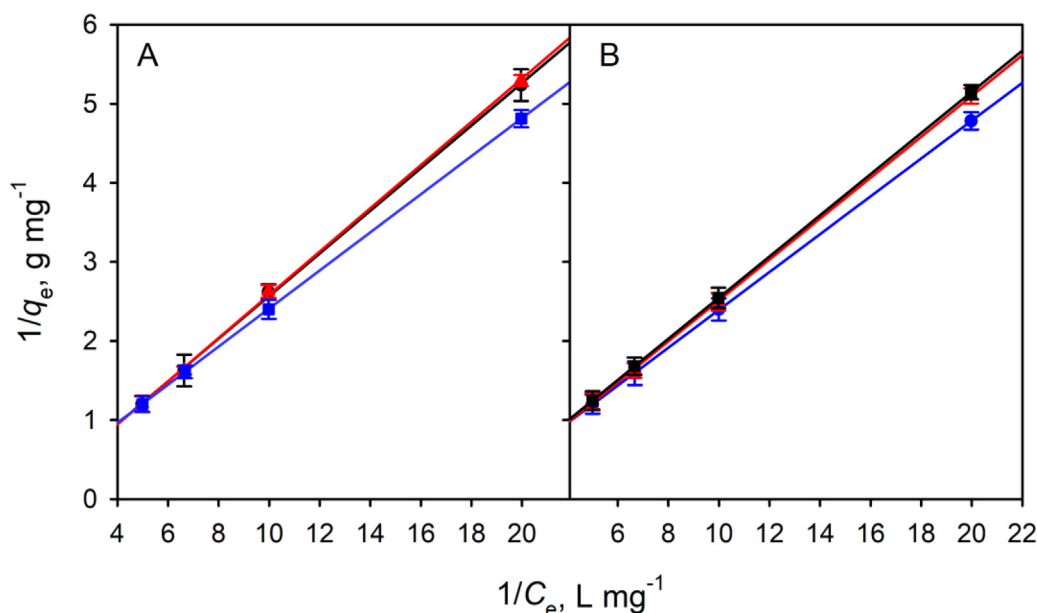


Fig. 5. Langmuir isotherm plots for adsorption of As(III) (A) and As(V) (B) onto Fe_3O_4 at temperatures 293 K (black), 303 K (red), and 323 K (blue). Isotherm corresponding to 293 K coincides with that of 303 K. The solid lines represent the fit of Eq. (1) to the data. Langmuir constants K_L are calculated from the linear fits. Error bars correspond to the standard deviation of three determinations.

Table 3

Fitting results of Eq. (1) to experimental data q_e and C_e for temperatures 293, 303 and 323 (data corresponding to $T = 343$ K match those of $T = 323$ K), showing R^2 and χ^2 values, and Langmuir constants K_L .

T (K)	As(III)		K_L (L mg ⁻¹)	As(V)		K_L (L mg ⁻¹)
	R^2	χ^2		R^2	χ^2	
293	0.99927	2.4×10^{-4}	0.0041	1	1.1×10^{-7}	0.0025
303	0.99934	2.1×10^{-4}	0.0046	0.9998	5.4×10^{-5}	7.06×10^{-4}
323	1	4.93×10^{-10}	0.0136	1	4.9×10^{-9}	0.0089

obtained are much smaller for Langmuir isotherm compared with Freundlich and Temkin ones, and Origin draws the conclusion automatically.

The evaluation of the standard Gibbs free energy ΔG^0 (kJ mol⁻¹) classifies the adsorption process as chemisorption, physisorption, or a combination of both [19]. In order to obtain a spontaneous adsorption, negative ΔG^0 values are mandatory, physisorption lying within the range [-20, 0] kJ mol⁻¹, and chemisorption within [-400, -80] kJ mol⁻¹. The range in between can be labelled as a physicochemical adsorption. For each temperature, the ΔG^0 value is:

$$\Delta G^0 = -RT \ln(K_t) \quad (2)$$

where R is the gas constant, T is the temperature, and K_t is the equilibrium thermodynamic constant, which value should be properly determined from the Langmuir constant K_L at each T , transforming K_L into the adimensional variable K_t [20]:

$$K_t = \frac{1000 \cdot K_L \cdot M \cdot [\text{adsorbate}]^0}{\gamma} \quad (3)$$

In Eq. (3), $[\text{adsorbate}]^0 = 1 \text{ mol L}^{-1}$ represents the standard concentration of the adsorbate, M is the molecular mass of the adsorbate (g mol⁻¹), and $\gamma = 1$ denotes the activity coefficient of the dilute solution. The results for temperatures 293, 303, 323 and 343 K yield ΔG^0 values within the range [-23.13, -12.83], close to the limit of a physisorption, but that can be considered as a combination of physical and chemical

adsorption, a common feature for the adsorption of some metal ions onto magnetic nanoparticles [21].

3.5. Study of competition with other ions present in water and application to real water samples

Drinking water, waste water and, in general, water from any source contain numerous dissolved ions in high concentrations. In order to verify that the method proposed in this work is not affected by the presence of these other important ions in water, the procedure was carried out by adding to the aqueous medium high concentrations (500 and 1000 mg L⁻¹) of Ca^{2+} , Pb^{2+} , Hg^{2+} , Mg^{2+} , Cl^- , NO_3^- and SO_4^{2-} in the presence of 50 $\mu\text{g L}^{-1}$ of arsenic. The study was carried out by measuring the arsenic concentrations before and after the adsorption process in the presence of the possible interfering species individually. The results showed that the As elimination process was not affected in any case. Therefore, the proposed method could be applied to any water containing these common ions, even in high concentrations. The study of the presence of potential interfering species has been extended to the use of lower arsenic concentrations, even below 10 $\mu\text{g L}^{-1}$. In this case, as the direct determination of arsenic is not possible, we have used a microextraction procedure previously developed by us [22] that allows speciation. With this procedure, an enrichment factor of 98 is achieved, which allows us to reach the necessary sensitivity to detect arsenic concentrations before and after the removal process. Using this procedure, we have found that the above-mentioned species do not cause deviations of more than 2% in the total arsenic recovery.

In addition, this method for the removal of As(III) and As(V) in water was applied to real water samples, which have a more complex matrix that could affect the removal process. Table 4 shows the results obtained for three river water samples and two drinking water samples (initially free of As) spiked with 50 $\mu\text{g L}^{-1}$ As(III) and As(V), respectively, to which the procedure was applied. To measure the low concentrations of arsenic remaining in solution after the removal process, we have applied a dispersive solid-phase microextraction procedure [22].

As shown in the table above, the As removal efficiency was above 99% in all cases, so the matrix of these real water samples does not affect the method presented in this work.

Table 4

Application of the arsenic removal procedure to water samples from different sources.

Water Sample	[As] found	[As] added, $\mu\text{g L}^{-1}$	Removal efficiency ^a , %
River 1	≤ LOD	100	99.2 ± 0.6
River 2	≤ LOD	100	99.1 ± 1.1
River 3	≤ LOD	100	99.5 ± 0.9
Drinking water 1	≤ LOD	100	99.3 ± 1.3
Drinking water 2	≤ LOD	100	99.3 ± 0.5

^a mean value ± standard deviation of three determinations; LOD = 5 $\mu\text{g L}^{-1}$.

4. Conclusion

This work presents a novel method for the complete and instantaneous removal of As(III) and As(V) from water, considered a major environmental pollutant, by the in situ formation of magnetic Fe_3O_4 nanoparticles. The Fe_3O_4 precursors are added directly to water containing inorganic arsenic and these species are adsorbed onto the nanoparticles as they form. This phenomenon gives the process an unprecedented speed for the complete removal of As from water. The Fe_3O_4 precursors are inexpensive chemical reagents and the adsorbent can be quickly removed from the aqueous medium using a magnet, making this simple method an alternative to conventional methods with low volume of sample treated. Studies are now in progress in order to apply to larger water samples for the purpose to reduce the amount of reagents used. Furthermore, this process has been successfully applied to real water samples without loss of removal efficiency.

Since the proposed methodology requires the use of a basic medium (pH=8) to achieve ferrite formation and retention of the arsenic forms, this may be a limiting point from the point of view of practical application of the methodology. With this in mind, we are continuing to work to achieve arsenic retention under experimental conditions that are easily transferable to conventional purification systems.

Funding

The authors acknowledge the financial support of the Spanish MCIN (Project PID2021–123201NB-I00 financed by MCIN/AEI/10.13039/501100011033/FEDER, UE).

Declaration of Competing Interest

The authors declare that the work described has not been published previously, that it is not under consideration for publication elsewhere and that this publication is approved by all authors

CRedit authorship contribution statement

Yesica Vicente-Martínez: Conceptualization, Methodology, Investigation, Writing – original draft, Supervision, Writing – review & editing. **Manuel Caravaca:** Methodology, Data curation, Writing – original draft, Writing – review & editing. **Sokaina El Farh:** Conceptualization, Investigation, Writing – review & editing. **Manuel Hernández-Córdoba:** Writing – review & editing, Supervision, Funding acquisition. **Ignacio López-García:** Investigation, Data curation, Writing – review & editing.

Data availability

No data was used for the research described in the article.

Acknowledgments

The authors acknowledge the financial support of the Spanish MICINN (PID2021–123201NB-I00). Moreover, the authors want to

thank the University Centre of Defence at the Spanish Air Force Academy, MDE-UPCT.

References

- [1] I. Ahmad, A. Ghaffar, A. Zakir, Z.U. Khan, M.F. Saeed, et al., Activated biochar is an effective technique for arsenic removal from contaminated drinking water in Pakistan, *Sustainability* 14 (21) (2022), doi:10.3390/su142114523.
- [2] A.K. Meher, S. Das, S. Rayalu, A. Bansiwani, Enhanced arsenic removal from drinking water by iron-enriched aluminosilicate adsorbent prepared from fly ash, *Desalination* 374 (2016) 20944–20956, doi:10.1080/19443994.2015.1112311.
- [3] W.H. Organization, Guidelines for drinking-water quality Fourth Edition Incorporating the First Addendum, W.H. Organization, 2017 <https://apps.who.int/iris/bitstream/handle/10665/254637/9789241549950-eng.pdf> Accessed 24 March 2023.
- [4] S.H. Frisbie, E.J. Mitchell, Arsenic in drinking water: an analysis of global drinking water regulations and recommendations for updates to protect public health, *PLoS One* 17 (4) (2022) e0263505, doi:10.1371/journal.pone.0263505.
- [5] G. Abbas, B. Murtaza, I. Bibi, M. Shahid, N.K. Niazi, et al., Arsenic uptake, toxicity, detoxification, and speciation in plants: physiological, biochemical, and molecular aspects, *Int. J. Environ. Res. Public Health* 15 (1) (2018), doi:10.3390/ijerph15010059.
- [6] S.T. McBeath, A. Hajimalayeri, S.Y. Jasim, M. Mohseni, Coupled electrocoagulation and oxidative media filtration for the removal of manganese and arsenic from a raw ground water supply, *J. Water Process. Eng.* 40 (2021), doi:10.1016/j.jwpe.2021.101983.
- [7] M.A. Hashim, A. Kundu, S. Mukherjee, Y.S. Ng, S. Mukhopadhyay, et al., Arsenic removal by adsorption on activated carbon in a rotating packed bed, *J. Water Process. Eng.* 30 (2019), doi:10.1016/j.jwpe.2018.03.006.
- [8] T. Siddique, R. Balu, J. Mata, N.K. Dutta, N.R. Choudhury, Electrospun composite nanofiltration membranes for arsenic removal, *Polymers* 14 (10) (2022) Basel, doi:10.3390/polym14101980.
- [9] S. Leaper, E.O.A. Caceres, J.M. Luque-Alled, S.H. Cartmell, P. Gorgojo, POSS-functionalized graphene oxide/PVDF electrospun membranes for complete arsenic removal using membrane distillation, *ACS Appl. Polym. Mater.* 3 (4) (2021) 1854–1865, doi:10.1021/acsapm.0c01402.
- [10] H. Salehi, A.A. Ebrahimi, M.H. Ehrampoush, M.H. Salmani, R.F. Fard, et al., Integration of photo-oxidation based on UV/Persulfate and adsorption processes for arsenic removal from aqueous solutions, *Groundw. Sustain. Dev.* 10 (2020), doi:10.1016/j.gsd.2020.100338.
- [11] T.K. Das, T.S. Sakthivel, A. Jeyaranjan, S. Seal, A.N. Bezbaruah, Ultra-high arsenic adsorption by graphene oxide iron nanohybrid: removal mechanisms and potential applications, *Chemosphere* 253 (2020), doi:10.1016/j.chemosphere.2020.126702.
- [12] W.T. Fu, D.L. Lu, H. Yao, S.J. Yuan, W. Wang, et al., Simultaneous roxarsone photocatalytic degradation and arsenic adsorption removal by $\text{TiO}_2/\text{FeOOH}$ hybrid, *Environ. Sci. Pollut. Res.* 27 (15) (2020) 18434–18442, doi:10.1007/s11356-020-08310-5.
- [13] I. López-García, Y. Vicente-Martínez, M. Hernández-Córdoba, Speciation of silver nanoparticles and Ag(I) species using cloud point extraction followed by electrothermal atomic absorption spectrometry, *Spectrosc. Acta Pt. B Atom. Spectr.* 101 (2014) 93–97, doi:10.1016/j.sab.2014.07.017.
- [14] G.E. Lloyd, Atomic-number and crystallographic contrast images with the SEM - a review of backscattered electron techniques, *Mineral. Mag.* 51 (359) (1987) 3–19, doi:10.1180/minmag.1987.051.359.02.
- [15] N.M. Otiniano, M. de la Cruz-Noriega, L. Cabanillas-Chirinos, S. Rojas-Flores, M.A. Munoz-Rios, et al., Arsenic biosorption by the macroalgae *Chondracanthus chamissoi* and *Cladophora* sp., *Processes* 10 (10) (2022), doi:10.3390/pr10101967.
- [16] Y. Vicente-Martínez, M. Caravaca, A. Soto-Meca, Non-chromatographic speciation of arsenic by successive dispersive liquid-liquid microextraction and in situ formation of an ionic liquid in water samples, *Microchem. J.* 157 (2020), doi:10.1016/j.microc.2020.105102.
- [17] F. Yu, Y. Li, G. Huang, C. Yang, C. Chen, et al., Adsorption behavior of the antibiotic levofloxacin on microplastics in the presence of different heavy metals in an aqueous solution, *Chemosphere* 260 (2020), doi:10.1016/j.chemosphere.2020.127650.
- [18] Y. Vicente-Martínez, M. Caravaca, A. Soto-Meca, M.A. Martín-Pereira, M. del Carmen García-Onsurbe, Adsorption studies on magnetic nanoparticles functionalized with silver to remove nitrates from waters, *Water* 13 (13) (2021) Basel, doi:10.3390/w13131757.
- [19] M. Caravaca, Y. Vicente-Martínez, A. Soto-Meca, E. Angulo-Gonzalez, Total removal of amoxicillin from water using magnetic core nanoparticles functionalized with silver, *Environ. Res.* 211 (2022) 113091–113091, doi:10.1016/j.envres.2022.113091.
- [20] P.S. Ghosal, A.K. Gupta, Determination of thermodynamic parameters from Langmuir isotherm constant-revisited, *J. Mol. Liq.* 225 (2017) 137–146, doi:10.1016/j.molliq.2016.11.058.
- [21] Y. Vicente-Martínez, M. Caravaca, A. Soto-Meca, Simultaneous adsorption of mercury species from aquatic environments using magnetic nanoparticles coated with nanomeric silver functionalized with L-cysteine, *Chemosphere* 282 (2021), doi:10.1016/j.chemosphere.2021.131128.
- [22] I. López-García, J.J. Marin-Hernández, M. Hernández-Córdoba, Magnetic ferrite particles combined with electrothermal atomic absorption spectrometry for the speciation of low concentrations of arsenic, *Talanta* 181 (2018) 6–12, doi:10.1016/j.talanta.2017.12.086.